

Chapter 39

Numerical Simulations of the Cutting Forces in an End Milling Process with Process Damping, Tool Runout and Variable Pitch Effects



C. Trivikrama Raju, S. Jakeer Hussain, and G. Yedukondalu

Abstract Milling cutters with runout, process dampening, and variable pitch did not solve milling difficulties because they did not address the regenerative chatter mechanism. When the phase difference between two waves varies from tooth to tooth, it throws off the regeneration process. The focus of this study is on devising a quick and accurate technique to quantify these influences during end milling. To enhance production quality and process stability while decreasing tool wear and machining costs, these methods may be included into an adaptive model for managing cutting force. The simulation results show that the cutting forces in end milling are small as compared to conventional scale cutting. In this study, an alternative process damping model has been presented for end milling based on an equivalent viscous damping approach. Furthermore, the technique is used to investigate how different tool geometries affect stability tendencies in variable pitch milling. Some novel phenomena are shown and discussed for certain parameter combinations.

39.1 Introduction

Major technological advances have been achieved in the field of high-speed machining (HSM). Better spindle designs allow for speeds of 30k and higher in micro-milling. Increasing the spindle speed and depth of cut during machining increases the rate of material removal. Nevertheless, high speed machining at larger depths of cut is hindered by the chatter phenomenon, which results in machining process to

C. Trivikrama Raju · G. Yedukondalu

Department of Mechanical Engineering, Koneru Lakshmaiah Education Foundation, Vaddeswaram, Guntur, India

S. Jakeer Hussain (✉)

Department of Mechanical Engineering, Mother Teresa Institute of Science and Technology, Sathupally, India

e-mail: jakeershaik786@gmail.com

be instable leading to unsatisfactory finish of the surface and potentially destroying the life of the cutting tool and work pieces. Driven by the current needs of highly automated production, the recognition of higher-productive, higher-quality, low-cost milling necessitates the concern of exact cutting force and chatter models. These days, the primary instruments used in manufacturing are stability lobe diagrams, which visually distinguish stable cutting circumstances from unstable or chatter ones. Using the tool point frequency response function (FRF), tool geometry, cutting factors, and cutting force coefficients, Altintas and Budak [1] demonstrated the models necessary to forecast the stability lobes. Several studies on the milling process parameters related to the chatter studies have been the subject of a number of previous research, including those by Altintas and Weck [2], Bravo et al. [3], Gagnola et al. [4] and Tanga et al. [5] inverse analysis of the self-excited chatter vibration has been recently reported, and it has been used by Suzuki et al. [6] to build a novel method for calculating the transfer function. The accuracy of the SLD was refined by Raphael et al. [7], who also investigated how the spindle's electronic position and velocity affected SLD accuracy. Lin and Tu [8], Jiang and Zhang [9], Penga et al. [10], Cao et al. [11], Gao and Meng [12] and a few more publications deal with the design of end mill spindles and identify the design elements that largely affect the stability lobe diagrams of these tools. Effects such as bearing preload on the tip of the tool frequency responses were studied by the Ozturk et al. [13]. Preload and spindle speed were shown to have a correlation in the examined instance. A dynamic model of high-speed motorised spindles was investigated by Liu and Chen [14]. To conduct a design sensitivity analysis, a design flowchart is drawn up. In the past, academics have attempted to optimise the milling process by taking a number of variables into account. To improve machining performance, Altintas [15] used simulated annealing and a genetic algorithm, two artificial computing approaches. Experimental investigations verify the combined use of the two methods. In order to foretell the cutting forces in an end milling operation, Jalili Saffar and Razfar [16] created a 3D modelling of the cutting forces are optimised using a genetic algorithm approach and then verified experimentally. Mathematics modelling the interaction between machining dynamics and material behaviour was developed by Palanisamy et al. [17]. The cutting process settings and tool vibration levels are optimised to save machining time using a robust GA approach. Using particle swarm optimization, Hsieh and Chu [18] created a generative tool path in a five axis milling machine using PSO algorithm. Using proactive and well-informed PSOs improves search efficiency. The harmony search (HS) technique was proposed by Zarei et al. [19] to determine face-milling parameters. The optimal depth of cut, feed rate, and cutting speed are achieved by a series of passes using a variety of machining settings in order to minimise the total cost of manufacturing.

Whereas optimum machining studies related to the cutting process is considered as a function of the geometric parameters of the integrated spindle tool unit are only few presented by the previous authors. In the current study, we aim to acquire the best cutting process conditions of the end milling process by taking into account a few critical parameters of the spindle-tool unit and the corresponding flexible body

dynamics. End-milling studies with the currently available parametric conditions confirm the accuracy of the machining process.

39.2 Modeling of Cutting Force Simulations

The workpiece is supposed to be stiff, whereas the tool is assumed to be flexible. Cutting process stability evaluation requires consideration of both tool geometry and machining requirements. The parameter like angle between each tooth, teeth numbers, helix angle of the tool, diameter of the tool and run-out are all part of the tool geometry. Spindle speed, axial depth of cut, feed per tooth, and entry/exit angles (a function of radial immersion) are required machining requirements. As b and $h(\phi_j)$ increase in the axial direction, the tangential and radial components of the linear cutting force operating on tooth j increase accordingly.

$$F_{t,j}(\phi) = K_t b h(\phi_j) \quad (39.1)$$

$$F_{r,j}(\phi) = K_r F_{t,j}(\phi) = K_r K_t b h(\phi_j) \quad (39.2)$$

where tangential shearing (K_t) and normal shearing (K_r) both contribute to the overall flute coefficient. Both the tangential and normal force components are projected onto the fixed (x, y) coordinate frame in the following ways:

$$F_{x,j} = -F_{t,j} \cos \phi_j - F_{r,j} \sin \phi_j \quad (39.3)$$

$$F_{y,j} = +F_{t,j} \sin \phi_j - F_{r,j} \cos \phi_j \quad (39.4)$$

By adding the sum across all the teeth (flutes), the total cutting forces may be calculated using the following closed-form expressions:

$$F_x(\phi) = \sum_{j=1}^{N_t} F_{x,j}; \quad F_y(\phi) = \sum_{j=1}^{N_t} F_{y,j} \quad (39.5)$$

39.2.1 Effects of Process Damping

Energy is dissipated in a process when a cutting tool's relief angle interacts with preexisting vibrations on the surface of the machined workpiece. Turning and milling are two processes where process damping has received a lot of attention from

researchers. It happens when the cutter’s flank touches with the imprinted vibrations on the cutting process. It may slow down the machining process and affect the dynamic cutting forces.

At the lower speeds of the spindle, the stability of the end milling are spaced closely and the chatter-free depths of cut are shown to decrease significantly. Fortunately, the chip width that may be used at low spindle speeds can be increased because to the process damping effect. The damping force for the milling force (F_d) is denoted by a 90° -phase shift with respect to the displacement, is of the negative sign to velocity component. Based on this information, the process damping force is described as the viscous damping force

$$F_d = -C \frac{b}{V} \dot{y} \tag{39.6}$$

Here, we define the y-direction process damping force and it is considered as the function of the velocity of the cutter (\dot{y}), cutting speed (v), width of the chip (b) and damping coefficient (C). The time-dependent cutting force direction is a major challenge in establishing an analytical solution for milling stability. The average force direction is considered together with the average tooth angle of the cut (f_{avg}). A time-independent or self-sufficient system may be built using this method. Initially, μ_x and μ_y are used to project the force in X and Y directions then, finally, the results are projected on to the normal of the surface. The milling process’s stability lobe boundaries may be calculated using the following equations:

$$b_{lim} = \frac{-1}{2K_s \text{Re}(H_{or}) N_t^*} \tag{39.7}$$

$$\frac{f_c}{\Omega N_t} = j + \frac{\varepsilon}{2\pi} \tag{39.8}$$

$$N_t^* = \frac{\phi_e - \phi_s}{360/N_t} \tag{39.9}$$

$$\varepsilon = 2\pi - 2 \tan^{-1} \left(\frac{\text{Re}[H_{or}]}{\text{Im}[H_{or}]} \right) \tag{39.10}$$

$$H_{or} = \mu_x H_x + \mu_y H_y \tag{39.11}$$

where, count of the teeth is represented as N_t , H_{or} is considered as oriented frequency response at the tool tip, $j = 0, 1, 2, \dots$ is the lobe number, force angle (β) in degrees. The process damping force may be easily used for both vertical and horizontal milling operations. In Fig. 39.1, n represents the surface normal direction, which is used to establish the geometry for the up-milling operation.

The n-axis damping force of a process is projected onto the x-axis as

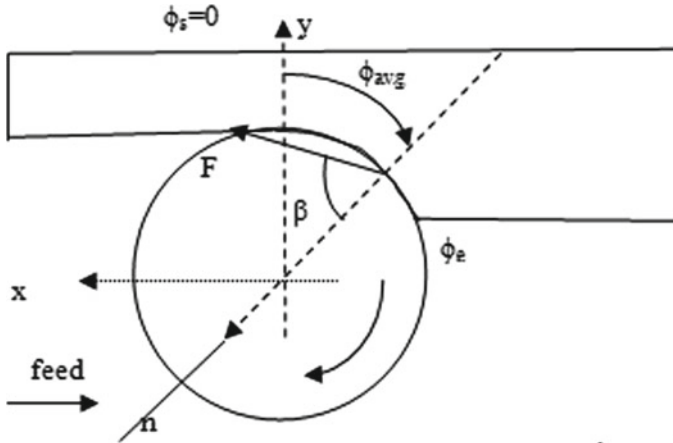


Fig. 39.1 Up-milling geometry based on the average tooth angle

$$F_x = F_d \cos(90 - \phi_{avg}) = -\left(C \frac{b}{V} \cos(90 - \phi_{avg})\right) \dot{n} \tag{39.12}$$

The damping force of a process is projected onto the x-axis as

$$F_x = -\left(C \frac{b}{V} \cos^2(90 - \phi_{avg})\right) \dot{x} \tag{39.13}$$

Therefore, the revised damping for x- and y-axis stability calculations is:

$$c_{new,x} = c_x + \left(C \frac{b}{V} \cos^2(90 - \phi_{avg})\right) \tag{39.14}$$

$$c_{new,y} = c_y + \left(C \frac{b}{V} \cos^2(180 - \phi_{avg})\right) \tag{39.15}$$

The damping values in the x and y directions are produced for down milling using the same method as outlined for up milling.

$$c_{new,x} = c_x + \left(C \frac{b}{V} \cos^2(\phi_{avg} - 90)\right) \tag{39.16}$$

$$c_{new,y} = c_y + \left(C \frac{b}{V} \cos^2(180 - \phi_{avg})\right) \tag{39.17}$$

39.2.2 Tool Run-Out and Cutting Force Modelling

When a mechanical system is in motion, tool run-out occurs when the tool is not perfectly aligned with the axis of rotation. The effect of the tool run-out is a serious problem in the machining process that may arise from a number of different sources, including misalignment between the tool holder and spindle, incorrect radial tooth location on the cutter, inaccurate tool dimensions, thermal tool deflection, improper tool and holder balance, and so on. As a result, the tool is subjected to unequal stresses across its cutting teeth at all times. Chip thickness varies as the tool rotates. The cutting forces were determined by the cutting geometry that was inserted into the workpiece, and the cutting forces were related to the uncut chip thickness using empirical formulae. The Eccentricity called as the run-out distance and the run cut angle (λ) characterize radial run-out. A circular approximation of the cutting tool's path allows us to use the following formula to get the chip thickness, which accounts for tool run-out.

$$h_j(\phi_j) = f_t \sin(\phi_j) + h_{ro}^j \quad (39.18)$$

Here we describe the chip thickness variation caused by run-out in cutting edge j as

$$h_{ro}^j = \rho_j - \rho_{j-1} \quad (39.19)$$

The cutting edge with run-out is the difference between the calculated and actual radii of each flute, which causes a shift in the cutting load. Run-out causes a difference between the nominal radius and the real radius, which is the radius along which the flute actually travels.

The effective radius variation along the cutting edge is not a significant factor when working with the tiny values of depth of cut and helix angle examined in this study, therefore the tool run-out is appropriately described by the difference between the actual and nominal trajectories for each flute. Cutting forces in the X and Y directions may be derived from the resolution of the tangential and radial forces, as the particular cutting force is a function of these three forces and the chip thickness along the cutting edge.

$$\begin{Bmatrix} F_{x,j}(\phi_j) \\ F_{y,j}(\phi_j) \end{Bmatrix} = \begin{bmatrix} -\cos(\phi_j) & -\sin(\phi_j) \\ \sin(\phi_j) & -\cos(\phi_j) \end{bmatrix} \begin{Bmatrix} F_{t,j} \\ F_{r,j} \end{Bmatrix} \quad (39.20)$$

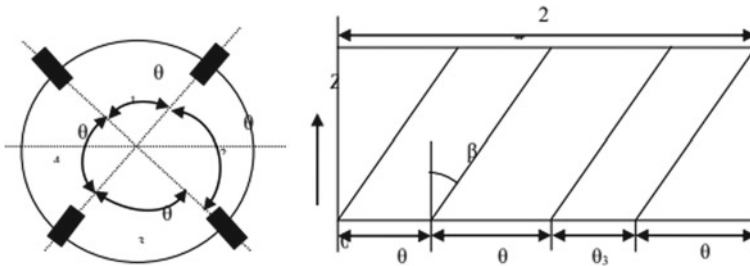


Fig. 39.2 Edge inclination on the end mill cutter's rim

39.2.3 Cutting Force Modelling Considering the Influence of Pitch

In most cases, it is believed that the cutter's teeth are evenly spaced (i.e., have a consistent tooth pitch) throughout its rim. When milling tough materials, it's common practice to use a tool with a variable pitch end mill. Mills with a tunable pitch angle may also have a tunable helix angle. Figure 39.2 depicts how the feed per tooth of a variable pitch tool changes as a function of the tooth angle θ_i (degrees).

The feed per tooth ratio is evaluated as given below

$$f_{t,variable} = \left[\frac{f_{t,mean} \times \theta_i \times N_t}{360^\circ} \right] \tag{39.21}$$

where $f_{t,mean}$ is the mean feed per tooth and N_t is the number of teeth.

39.3 Results and Discussions

Using the information in Table 39.1, a Matlab programme depicts the stability lobe diagram of the frequency response function of the tool tip.

Coefficients of the system's modal and cutting modes are listed in Table 39.1.

Table 39.1 System's modal parameters and cutting force coefficients

Cutting tool parameters	Numerical values
Cutting stiffness in X and Y directions	2.1×10^8 N/m
Natural frequency ($\omega_x = \omega_y$)	2056 Hz
Damping ratio ($\xi_x = \xi_y$)	0.01
Diameter of the tool	12 mm
Specific cutting pressure (K_s)	750 N/mm^2
Total tooth of the cutter (N_t)	4

To examine the impact of process damping with these updates to the classical model, a MATLAB programme is constructed. The radial immersion ratio of 50% is used in the numerical analysis. With the data obtained from finite element analysis approach, the frequency responses are arrived and it is further utilized to plot the stability areas for the up-milling operation are displayed. Stability charts for varying the process damping constant from zero (no process damping) to the highest value ($C = 6.5 \times 10^5$ N s/m) are shown in Fig. 39.3. The average steady depth of cut is found to rise from 0.04 to 0.3 mm when the process is dampened.

In order to simulate the cutting force, modal parameters, the tool shape, and machining requirements must be provided. Each mode of the tool in the x and y axes has its own set of modal characteristics, which include its stiffness, damping ratio, and natural frequency. In Fig. 39.4, we see the results of a time-domain simulation of a milling model with two degrees of freedom, both with and without the influence of process damping. When the process damping effect is included into the model, it is shown that the x and y levels of tool displacements decrease. In addition, it offers the constant tool displacements that are crucial for a consistent cut.

A tool with a 12 mm diameter is used to demonstrate the impact of run-out. Run-out is typically measured along the feed direction. For the case of a run-out offset of 10 μm , simulations are performed in the time domain both with and without run-out effects, as shown in Fig. 39.5. The cutting process is modelled in two dimensions, and all spindle-tool system characteristics are taken into account.

The amounts of tool displacement are shown to rise as run-out increases throughout the cutting process. The cutting pressures experienced by the virtual

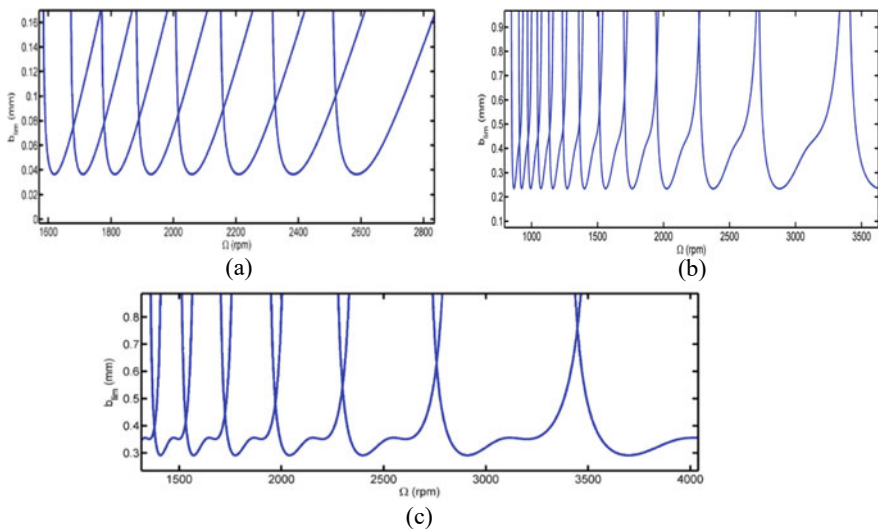


Fig. 39.3 Analytical stability lobe diagrams. **a** In the absence of process dampening, **b** in the presence of process dampening with $C = 6.5 \times 10^4$ N s/m, **c** in the presence of process dampening with $C = 6.5 \times 10^5$ N s/m

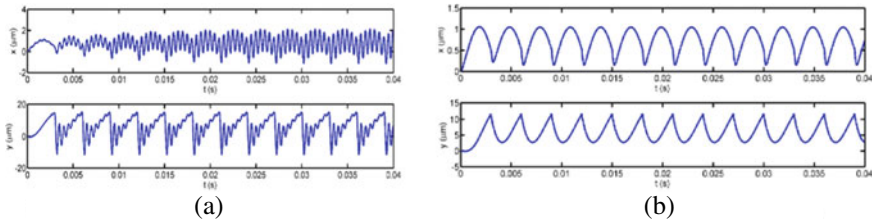


Fig. 39.4 Vibrations from the cutter at a depth of 1 mm and spindle speed of 3000 rpm. **a** In the absence of process dampening, **b** presence of process dampening with $C = 6.5 \times 10^5$ N s/m

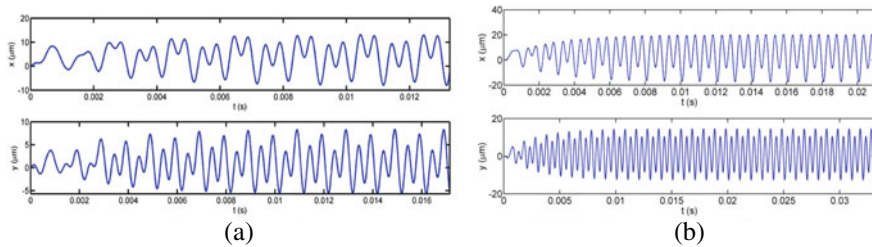


Fig. 39.5 Run-out correction levels for tool displacements. **a** In the absence of run-out, **b** in the presence of run-out

tool for run-out values of 10 and 25 μm are shown in Fig. 39.6. As can be seen in Fig. 39.6, the cutting forces for each flute vary by just a little amount (10–12 μm). Cutting forces may be detected with significant amplitude in the variations in load of the chip at each tooth is shown in Fig. 39.6b, leading to unacceptable vibration levels of the tool as cutting progresses.

Using a tool with variable pitch spacing [0 95 180 275] degrees and with equal pitch [0 90 180 270] degrees for two different axial depths of cut, Fig. 39.7 displays the observed resulting forces with a 25% immersion of the radial cut in up-milling of aluminum alloy. It is seen that the forces fluctuate non-linearly due to the varied

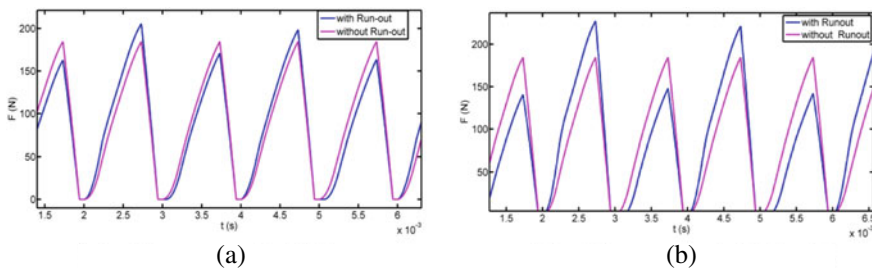


Fig. 39.6 Force variations as a result of tooth wear. **a** With a run-out of 10 μm , **b** with a run-out of 25 μm

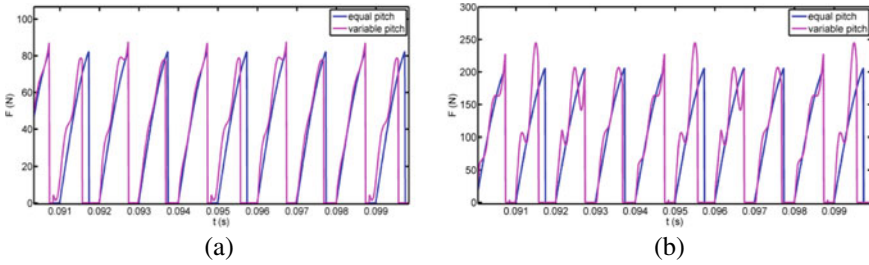


Fig. 39.7 Variable-pitch time-domain simulation at 25% radial immersion. **a** Cutting depth = 1 mm, **b** cutting depth = 2.5 mm

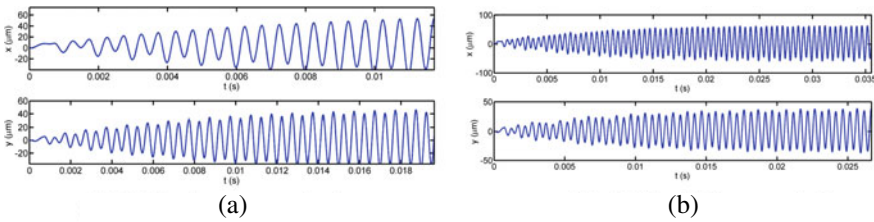


Fig. 39.8 Vibration levels of tools at 1 mm depth of cut. **a** With the same pitch, **b** with different pitch

pitch as the axial depth of the cut raised from 1 to 2.5 mm, the cutting forces also have been raised significantly.

At an axial depth of cut as 1 mm example with as equivalent and varied pitch of the tool, the cutting tool displacement values are achieved as illustrated in Fig. 39.8. The cutting tool’s variable pitch clearly raises the displacement levels of the tool dramatically.

39.4 Conclusions

As a result, evaluating the cutting process’s stability demands an ideal selection of cutting tool settings with regard to those factors. Errors in machining may arise from a number of different factors, including tool run-out, tool deflection, workpiece displacements, and variable pitch end mills. There are situations when the procedure fails despite having a well-designed spindle and tool. The aforementioned calculations allow one to determine the maximum allowable tool run-out in terms of spindle dimensions. For the proposed spindle-tool configuration, tools with variable pitches are also permitted for use during machining to achieve the greater stable depth of cuts. In an integrated spindle-tool spindle system, the damping force at the interface regions such as collet and tool, chuck and the collet are having a major impact on

the system's stability, process damping has an effect analogous to that of the internal damping. In order to guarantee the steadiness of the cutting process, the findings shown that the proposed approach may be utilized for accurate assessment of tool run-out, process damping, and variable pitch effects.

References

1. Altintas, Y., Budak, E.: Analytical prediction of stability lobes in milling. *Ann. CIRP* **44**, 357–362 (1995)
2. Altintas, Y., Weck, M.: Chatter stability of metal cutting and grinding. *CIRP Ann. Manf. Technol.* **53**, 619–642 (2004)
3. Bravo, U., Altuzarra, O., Lopez de Lacalle, L.N., Sanchez, J.A., Campa, F.J.: Stability limits of milling considering the flexibility of the workpiece and the machine. *Int. J. Mach. Tools Manf.* **45**, 1669–1680 (2005)
4. Gagnola, V., Bouzgarrou, B.C., Raya, P., Barra, C.: Model-based chatter stability prediction for high-speed spindles. *Int. J. Mach. Tools Manf.* **47**, 1176–1186 (2007)
5. Tanga, W.X., Songa, Q.H.: Prediction of chatter stability in high-speed finishing end milling considering multi-mode dynamics. *Int. J. Mach. Tools Manuf.* **209**, 2585–2591 (2009)
6. Suzuki, N., Kurata, Y., Kato, T., Hino, R., Shamoto, E.: Identification of transfer function by inverse analysis of self-excited chatter vibration in milling operations. *Precis. Eng.* **36**, 568–575 (2012)
7. Raphael, G.S., Reginaldo, T.C.: A contribution to improve the accuracy of chatter prediction in machine tools using the stability lobe diagram. *J. Manuf. Sci. Eng. ASME*. **136**, 021005–021007 (2014)
8. Lin, C.W., Tu, J.F.: Model-based design of motorized spindle systems to improve dynamic performance at high speeds. *J. Manuf. Process.* **9**, 94–108 (2007)
9. Jiang, S., Zheng, S.: Dynamic design of a high-speed motorized spindle-bearing system. *J. Mech. Des. ASME* **132**, 0345011–0345015 (2010)
10. Penga, Z.K., Jackson, M.R., Guo, L.Z., Parkin, R.M., Meng, G.: Effects of bearing clearance on the chatter stability of milling process. *Nonlinear Anal. Real World Appl.* **11**, 3577–3589 (2010)
11. Cao, H., Holkup, T., Altintas, Y.: A comparative study on the dynamics of high speed spindles with respect to different preload mechanisms. *Int. J. Mach. Tools Manuf.* **57**, 871–883 (2011)
12. Gao, S.H., Meng, G.: Research of the spindle over hang and bearing span on the system milling stability. *Arch. Appl. Mech.* **81**, 1473–1486 (2011)
13. Ozturk, E., Kumar, U., Turner, S., Schmitz, T.: Investigation of spindle bearing preload on dynamics and stability limit in milling. *Int. J. Mach. Tools Manuf.* **61**, 343–346 (2012)
14. Liu, J., Chen, X.: Dynamic design for motorized spindles based on an integrated model. *Int. J. Adv. Manuf. Technol.* **71**, 1961–1974 (2014)
15. Altintas, Y.: Modeling approaches and software for predicting the performance of milling operations at Mal-Ubc. *Mach. Sci. Technol.: Int. J.* **4**, 3445–3478 (2000)
16. Jalalli Saffar, R., Razfar, M.R.: Simulation of end milling operation for predicting cutting forces to minimize tool deflection by genetic algorithm. *Mach. Sci. Technol.: Int. J.* **14**, 81–101 (2010)
17. Palanisamy, P., Rajendran, I., Shanmugasundaram, S.: Optimization of machining parameters using genetic algorithm and experimental validation for end-milling operations. *Int. J. Adv. Manuf. Technol.* **32**, 644–655 (2007)
18. Hsieh, H.T., Chu, C.H.: Improving optimization of tool path planning in 5-axis flank milling using advanced PSO algorithms. *Robot. Comput.-Integr. Manuf.* **29**, 3–11 (2013)
19. Zareia, O., Fesanghary, M., Farshi, B., Saffar, J., Razfar, R.M.R.: Optimization of multi-pass face-milling via harmony search algorithm. *J. Mater. Process. Technol.* **209**, 2386–2392 (2009)